Biochem. J. (2012) **447**, 239–248 (Printed in Great Britain) doi:10.1042/BJ20120172

Dedifferentiated follicular granulosa cells derived from pig ovary can transdifferentiate into osteoblasts

Yoshinao OKI, Hiromasa ONO, Takeharu MOTOHASHI, Nobuki SUGIURA, Hiroyuki NOBUSUE and Koichiro KANO[1]

Laboratory of Cell and Tissue Biology, College of Bioresource Sciences, Nihon University, 1866 Kameino, Fujisawa 252-0880, Japan

Transdifferentiation is the conversion of cells from one differentiated cell type into another. How functionally differentiated cells already committed to a specific cell lineage can transdifferentiate into other cell types is a key question in cell biology and regenerative medicine. In the present study we show that porcine ovarian follicular GCs (granulosa cells) can transdifferentiate into osteoblasts *in vitro* and *in vivo*. Pure GCs isolated and cultured in Dulbecco's modified Eagle's medium supplemented with 20% FBS (fetal bovine serum) proliferated and dedifferentiated into fibroblast-like cells. We referred to these cells as DFOG (dedifferentiated follicular granulosa) cells. Microarray analysis showed that DFOG cells lost expression of GC-specific marker genes, but gained the expression of osteogenic marker genes during dedifferentiation. After osteogenic induction, DFOG cells underwent terminal osteoblast differentiation and matrix mineralization *in vitro*. Furthermore, when DFOG cells were transplanted subcutaneously into SCID mice, these cells formed ectopic osteoid tissue. These results indicate that DFOG cells derived from GCs can differentiate into osteoblasts *in vitro* and *in vivo*. We suggest that GCs provide a useful model for studying the mechanisms of transdifferentiation into other cell lineages in functionally differentiated cells.

Key words: dedifferentiated fat cell (DFAT cell), dedifferentiated follicular granulosa (DFOG), differentiation, osteoblast, ovary, transdifferentiation.

INTRODUCTION

Transdifferentiation is the conversion of cells from one differentiated type into another. It is particularly common in organisms such as urodele amphibians that exhibit regeneration of missing parts [1]. One well-known example is Wolffian lens regeneration in newts and salamanders. These amphibians can regenerate lost eye lenses through the transdifferentiation process that includes dedifferentiation, migration, proliferation and differentiation of the dorsal iris cells adjoining the lens [2]. Previously the molecular mechanism of transdifferentiation and several factors that directly regulate this process have been reported [3–5]. Transdifferentiation is rare in mammals, although cellular transdifferentiation has been demonstrated in an adult urodele amphibian [6,7]. A few accepted instances of transdifferentiation in mammals are the conversion of bovine vascular endothelium into smooth muscle [8] and pancreatic cells into hepatocytes in mice [9] and humans [10] *in vitro* and *in vivo*. However, whether these transdifferentiated cells undergo dedifferentiation, proliferation (cell cycle re-entry) and differentiation similar to that observed in the adult urodele amphibian is unclear.

We recently found that mature adipocytes can transdifferentiate into various cell types in mammals *in vitro* and *in vivo*. We also reported the establishment of multipotent progenitor cell lines, termed DFAT (dedifferentiated fat) cells, from mature adipocytes of various mammals including humans, pigs and rodents. DFAT cells possess long-term viability and differentiate into adipocytes, osteoblasts, chondrocytes, myoblasts and neuronal cells under appropriate conditions [11–14]. In our experiments, mature adipocytes dedifferentiated into DFAT cells and then differentiated into various cell types during transdifferentiation. We hypothesized that terminally differentiated cells can acquire multipotency during dedifferentiation. However, we have confirmed the multipotency of functionally differentiated cells only in mammalian adipocytes. Whether other functionally differentiated cells acquire multipotency similar to DFAT cells has not been elucidated to date. Investigation of the transdifferentiation ability of functionally differentiated cells other than adipocytes is important for understanding the universality of mammalian transdifferentiation.

During maturation of a primordial ovarian follicle into a pre-ovulatory follicle, various morphological and functional events occur inside the follicle. Among these events, differentiation of GCs (granulosa cells) plays a central role in follicle development. GCs have a multitude of specialized follicular functions, including secretion of large amounts of steroid hormones, adaptation of FSH (follicle-stimulating hormone) and luteinizing hormone receptivity to the endocrine milieu, and regulation of oocyte growth [15]. Hence, GCs are considered to be associated with functional differentiation. Ovarian follicles consist of follicular fluid, a single oocyte and several hundred thousand epithelial (membrana granulosa) cells inside a basement membrane. Because of this follicular structure, follicular-phase

Abbreviations used: ACAN, aggrecan; ALP, alkaline phosphatase; ALPL, ALP liver/bone/kidney; BMP, bone morphogenetic protein; BMSC, bone marrow stromal cell; BSP, bone sialoprotein; Cy3, indocarbocyanine; CYP11A1, cytochrome P450 family 11 subfamily A1; CYP19A3, cytochrome P450 family 19 subfamily A3; DAPI, 4′6-diamidino-2-phenylindole; DEX, dexamethasone; DFAT, dedifferentiated fat; DFOG, dedifferentiated follicular granulosa; DLX5, distal-less homeobox 5; DMEM, Dulbecco's modified Eagle's medium; FBS, fetal bovine serum; FSH, follicle-stimulating hormone; GAPDH, glyceraldehyde-3-phosphate dehydrogenase; GC, granulosa cell; GEO, Gene Expression Omnibus; IBSP, integrin-binding sialoprotein; INHBB, inhibin β B; LHCGR, luteinizing hormone/choriogonadotropin receptor; LIF, leukaemia-inhibiting factor; NR, nuclear receptor; OM, osteogenic medium; OSX, osterix; POU5F1, POU class 5 homeobox 1; RT, reverse transcription; RUNX2, Runt-related transcription factor 2; Sox9, SRY (sex determining region Y)-box 9; SPP1, secreted phosphoprotein 1; TC, theca cell.

[1] To whom correspondence should be addressed (email kkano@brs.nihon-u.ac.jp).

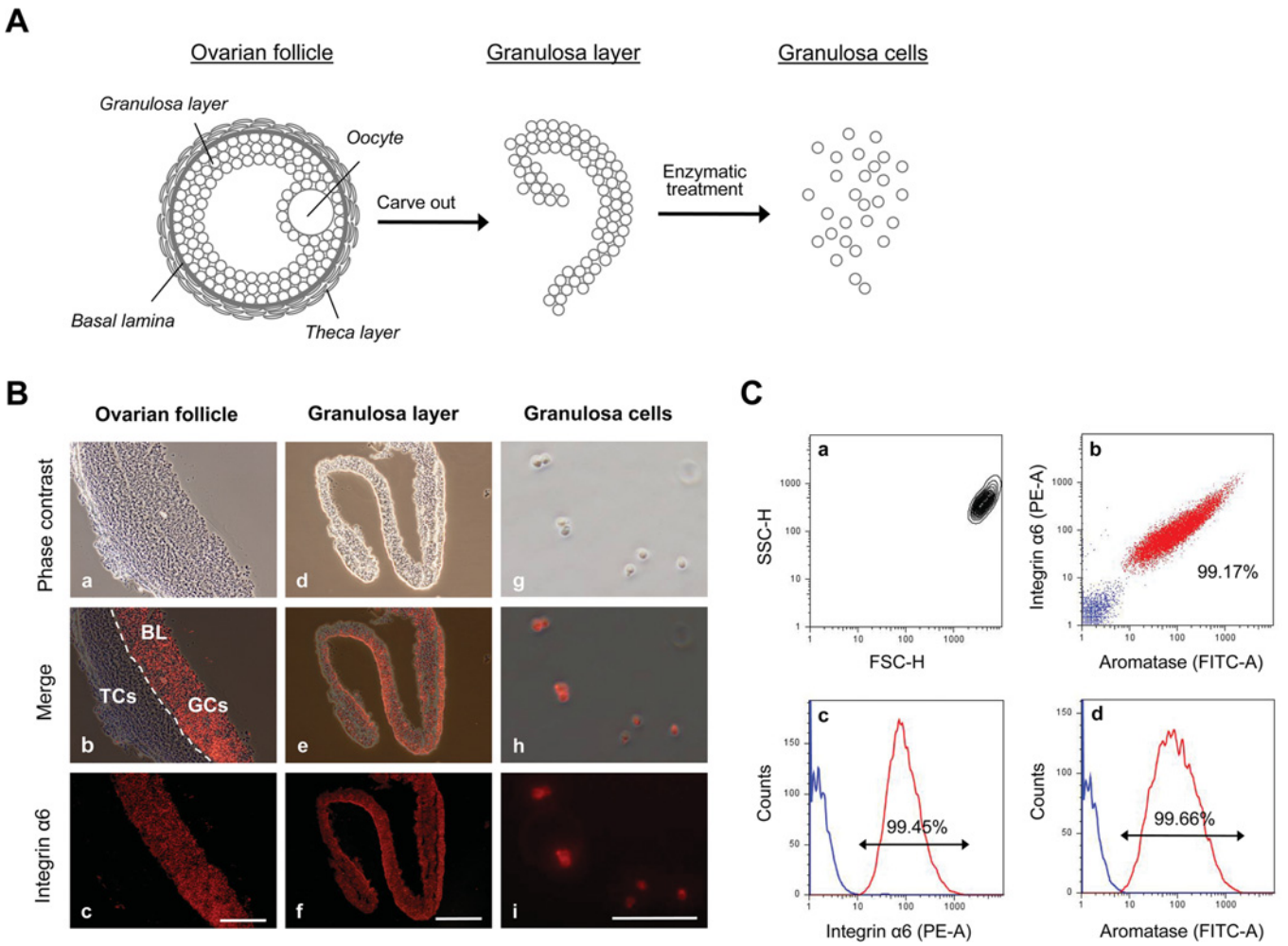

Figure 1 Isolation of homogeneous GCs from porcine ovarian follicles

(**A**) The granulosa layer was extracted from the ovarian follicle and digested with 0.1 % collagenase. After centrifugation, the isolated GCs were cultured in DMEM containing 20 % FBS for 7 days. During culture, the cells became attached to the dish and exhibited an extended morphology, followed by conversion into fibroblast-like DFOG cells. (**B**) Histological analysis of homogenous GCs from an ovarian follicle. a–c, GCs and TCs in ovarian follicles were distinguished by immunostaining with rat anti-(α6 integrin/CD49f) monoclonal antibody. In b, the broken lines indicate the basal lamina (BL). d–f, microscopic observations of the separated GC layer immunostained with rat anti-(α6 integrin/CD49f) monoclonal antibody. g–i, microscopic observations of isolated GCs immunostained with rat anti-(α6 integrin/CD49f) monoclonal antibody. The GC fraction consisted completely of α6 integrin/CD49f-positive cells; isolated cells were GCs. TCs and other cells were not observed. Scale bars = 100 μm. (**C**) FACS analysis of the GC fraction immunostained for the detection of α6 integrin/CD49f and cytochrome P450 aromatase. a, on contour diagrams, the forward scatter height (FSC-H) is plotted on the *x*-axis and the side scatter height (SSC-H) is plotted on the *y*-axis. The forward scatter height represents cell size, whereas side scatter height represents cell granularity. b, anti-(α6 integrin) phycoerythrin area (PE-A)/anti-(cytochrome P450 aromatase) fluorescein isothiocyanate area (FITC-A) double stain of the GC fraction. The population in red represents α6 integrin/cytochrome P450 aromatase-positive cells and that in blue represents integrin α6/aromatase-negative cells. c and d, on the trace, the phycoerythrin area and fluorescein isothiocyanate area are plotted on the *x*-axis, and the cell number (Counts) is plotted on the *y*-axis. The isolated cell fraction consisted of 99.17 % GCs.

GCs can be distinguished by their morphology and location *in situ* and can be easily isolated as a homogeneous cell population for *in vitro* analysis, similar to mature adipocytes [15]. Kossowska-Tomaszczuk et al. [16] reported that human-derived luteal phase GCs that grew in the presence of LIF (leukaemia-inhibiting factor) were differentiated into other cell lineages, such as osteoblasts, chondrocytes and neurons. Follicular-phase GCs are expected to be useful for clarifying the ability of mammalian differentiated cells to transdifferentiate into other functional cell types such as DFAT cells.

In the present study, we determined whether follicular-phase GCs transdifferentiate into osteoblasts in a manner similar to that exhibited by mature adipocytes. First, we demonstrated the purity of isolated porcine GCs by FACS and microscopic analysis. We found that isolated GCs begin to proliferate and dedifferentiate into fibroblast-like cells *in vitro*. We named these cells DFOG (dedifferentiated follicular granulosa) cells. Microarray analysis also showed that DFOG cells expressed not only stem cell markers, but also osteogenic markers during dedifferentiation. Furthermore, we showed that DFOG cells underwent terminal osteoblast differentiation, matrix mineralization *in vitro* and osteoid matrix formation following subcutaneous injection into the peritoneal cavity of SCID mice. We suggest that DFOG cells provide a useful model for studying the mechanisms of dedifferentiation and acquired multipotency of stem cells.

EXPERIMENTAL

Cell preparation

The primary porcine GC isolation method is illustrated in Figure 1(A). Porcine ovaries were obtained from Kanagawa

Meat Center (Kanagawa, Japan) and transported to the laboratory within 2 h. They were maintained in 0.9 % normal saline supplemented with penicillin G (100 units/ml) and streptomycin sulfate (0.2 mg/ml, Sigma) at 10–15 °C. In brief, antral follicles (4–6 mm in diameter) were excised from the ovaries and freed of the surrounding stromal tissues under a stereomicroscope (Olympus). GCs were isolated by a slight modification of a method described previously [17]. This involves puncturing and everting the follicle, followed by gentle stroking of the inner follicular wall with a pair of fine forceps to release sheets of GCs. The remaining follicular tissue (mainly theca) was discarded. Sheets of GCs were collected, washed three times in PBS (pH 7.4) by centrifugation at 300 ***g*** for 3 min at room temperature (20–24°C), and then digested with 0.1 % collagenase type II (Sigma–Aldrich) at 37 °C for 30 min. The digested cell suspension was then filtered through a 40-μm nylon mesh and centrifuged at 135 ***g*** for 3 min at room temperature. To determine whether all of the isolated cells were GCs, the primary cells were analysed by FACS (FACSCalibur, Becton Dickinson). The purity of GCs was assessed by immunostaining with rat anti-(α6 integrin/CD49f) monoclonal antibody (R&D Systems) [15] and mouse anti-(cytochrome P450 aromatase) antibody (AbD serotec). Rabbit anti-[rat IgG Cy3 (indocarbocyanine)-conjugated] affinity-purified antibody (Chemicon) and AlexaFluor 488 rabbit anti-(mouse IgG) (Molecular Probes) were used as secondary antibodies. The wavelengths used for fluorochrome emission were fluorescein isothiocyanate (525 nm) and phycoerythrin (575 nm). The percentage of positively stained cells was measured by FACS. Data acquisition and analysis were performed using Flowjo software (Tree Star).

A porcine sternum was obtained from Kanagawa Meat Center and transported to the laboratory within 2 h at 10–15 °C. In brief, bone marrow was harvested by flushing the sternum with DMEM (Dulbecco's modified Eagle's medium; Nissui Pharmaceutical) supplemented with 20 % (v/v) FBS (fetal bovine serum; Moregate BioTech) and 100 μg/ml kanamycin (Sigma–Aldrich). The pooled marrow was then placed in tissue culture dishes (BD Falcon 3001) containing DMEM supplemented with 20 % FBS and 100 μg/ml kanamycin and cultured for 96 h. Non-adherent cells were washed off, and adherent cells expanded until confluence (10 days).

Histological evaluation and immunostaining

Porcine organs were perfused with 4 % paraformaldehyde in PBS (Wako Pure Chemical) and frozen in Tissue-Tek OCT™ compound (Sakura). The specimens were cut into 4-μm-thick sections at −20 °C. They were then washed with PBS and incubated at room temperature for 1 h in 10 % normal goat serum (Vector Laboratories) in PBS to block non-specific binding of antibodies. Antigen retrieval and antibody staining were performed as per standard procedures. Rat anti-(α6 integrin/CD49f) monoclonal antibody was used as the primary antibody. To detect α6 integrin/CD49f, the cells were incubated at room temperature for 1 h with rabbit anti-rat IgG Cy3-conjugated affinity-purified antibody diluted 1:2000 in PBS. For immunofluorescence analysis of cells, the isolated primary GCs, DFOG cells and BMSCs (bone marrow stromal cells) were washed in Tris-buffered saline and fixed with 0.2 % Triton X-100 in zinc fix solution [0.1 M Tris (pH 7.4), 475 μg/ml calcium acetate, 5 mg/ml zinc acetate and 5 mg/ml zinc chloride in ultrapure water] overnight at 4 °C. The fixed cells were permeabilized with 0.2 % Triton X-100 in Tris-buffered saline for 30 min and washed in Tris-buffered saline. To block non-specific binding of antibodies, the cells were incubated at room temperature for 1 h in 10 % normal goat serum (Vector Laboratories) and 1 % BSA (Sigma–Aldrich) in Tris-buffered saline. After incubation in blocking buffer, antibody staining was performed as per standard procedures. The following primary antibodies were used to detect GC-specific markers: rat anti-(α6 integrin/CD49f) monoclonal antibody (dilution 1:50) and mouse anti-(cytochrome P450 aromatase) antibody (dilution 1:100). The following antibodies were used to detect osteogenic markers: mouse anti-(type 1 collagen) monoclonal antibody (AB1346, Chemicon). AlexaFluor 488 rabbit anti-(mouse IgG) (dilution 1:2000) and rabbit anti-(rat IgG Cy3-conjugated) affinity-purified antibodies (dilution 1:2000) were used as secondary antibodies. Antibodies were diluted in Tris-buffered saline with 1 % BSA. Cell nuclei were stained with Hoechst 33342 (5 μg/ml) in Tris-buffered saline. For immunohistochemical analysis of transplanted cells, tissue sections were deparaffinized, rinsed in Tris-buffered saline and immunochemical stained by M.O.M.™ kits (Vector Laboratories.). The following primary antibodies were used: mouse anti-(type 1 collagen) monoclonal antibody or anti-(bovine osteocalcin) monoclonal antibody (M041, TAKARA). The sections were stained with haematoxylin (Wako Pure Chemical) for histological analysis.

Dedifferentiation culture

Isolated GCs were placed in tissue culture dishes containing DMEM supplemented with 20 % (v/v) FBS and then incubated in a humidified atmosphere of 5 % CO_2. The medium was changed every 4 days until confluence (7 days).

Osteogenic induction

DFOG cells and BMSCs were placed in a tissue culture dish (BD Falcon 3001) containing DMEM supplemented with 20 % FBS and then incubated at 37 °C in a humidified atmosphere of 5 % CO_2. The medium was changed every 4 days until the cells were used. DFOG cells and BMSCs were grown to confluence for the differentiation experiments. Osteogenic differentiation of DFOG cells was induced by replacing the medium with DMEM supplemented with 10 % FBS, 10 μM all-*trans* retinoic acid (Sigma–Aldrich), 0.1 μM DEX (dexamethasone; Wako Pure Chemical) and insulin-transferrin-selenium-X supplement containing 5 μl/ml insulin (Invitrogen) and 10 mM 2-glycerophosphate (Wako Pure Chemical). After 96 h, the differentiation medium was replaced with DMEM supplemented with 10 % FBS containing 10 mM 2-glycerophosphate. Osteogenic differentiation of BMSCs was induced by replacing the medium with DMEM supplemented with 10 % FBS, 0.1 μM DEX, 50 μM ascorbic acid (Sigma) and 10 mM 2-glycerophosphate.

RNA extraction

Total RNA was extracted using TRIzol reagent (Invitrogen) and an RNeasy Mini kit (Qiagen) according to the manufacturer's instructions. RNA quality was assessed using a NanoDrop® ND-1000 UV–visible spectrophotometer (NanoDrop Technologies) and Agilent 2100 bioanalyser (Agilent Technologies).

Microarray analysis

Total RNA was isolated during dedifferentiation from GCs to DFOG cells at the following five time points: 0, 24, 48, 96 and 168 h. Isolation at each time point was performed in triplicate (i.e. biological replicates). The RNA samples were labelled using the GeneChip One-Cycle Target Labeling and Control Reagent

package (Affymetrix) and then hybridized to the Affymetrix GeneChip Porcine genome array according to the manufacturer's instructions. Fluorescent images were visualized using a GeneChip Scanner 3000 (Affymetrix). Expression and raw expression data (CEL files) were generated using GeneChip Operating System software (Affymetrix). The raw data were summarized and normalized using the Robust Multi-array Average algorithm and the Bioconductor package affy (http://www.bioconductor.org/packages/2.0/bioc/html/affy.html). The Spotfire DecisionSite for Functional Genomics software package (TIBCO Software) was used for visualization of microarray data. The raw and processed microarray data were deposited in NCBI's GEO (Gene Expression Omnibus) and are accessible through the GEO Series accession number GSE18854 (http://www.ncbi.nlm.nih.gov/geo/query/acc.cgi?acc=GSE18854).

RT (reverse transcription)–PCR

Gene expression levels were estimated by RT–PCR. Total RNA (500 ng) digested with DNase I was subjected to RT–PCR analysis. Total RNA was reverse transcribed using High Capacity RNA-to-cDNA Master mix (Applied Biosystems). Reverse transcripts were used as templates for analysing gene expression levels using AmpliTaq Gold PCR Master mix (Applied Biosystems) and a PX2 thermal cycler (Hybaid) according to the manufacturer's instructions. The following primer sets were used as GC-specific markers: *LHCGR* (luteinizing hormone/choriogonadotropin receptor) sense 5′-AAAGCACAGCAAGGAGACCA-3′ and antisense, 5′-TGAGGCAATGAGTAGCAGGTAGA-3′; *INHBB* (Inhibin β B) sense, 5′-TCTTCATCTCCAACGAGGGTAA-3′ and antisense 5′-TTCAGGTCCACACGCTTCTC-3′; and *CYP19A3* (cytochrome P450 19A3) sense, 5′-ATGAGGGTCTGGATAGGTGGAG-3′ and antisense, 5′-CAGGTGCTTGGTGATGGAA-3′. The following primer sets were used as osteogenic markers: *RUNX2* (Runt-related transcription factor 2) sense, 5′-CGAAATGCCTCTGCTGTTATG-3′ and antisense, 5′-TGCCTGGGGTCTGTAATCTC-3′; *SP7* transcription factor sense, 5′-GCTGTGAAACCTCAAGTCCTATGG-3′ and antisense, 5′-TCCAAGCCAATGTCCTCCTC-3′; *DLX5* (distal-less homeobox 5) sense, 5′-GCTACCGATTCCGACTACTACAGC-3′ and antisense, 5′-TTGCCGTTCACCATTCTCAC-3′; *SPP1* (secreted phosphoprotein 1) sense, 5′-TGATAGCCTTCTGCCTCTGG-3′ and antisense 5′-TCGTCCACATCGTCTGTTTG-3′; *ALPL* (alkaline phosphatase, liver/bone/kidney) sense, 5′-TCCAAGACATACAACACCAACG-3′ and antisense 5′-GTCACGATGCCCACAGATTT-3′; and *IBSP* (integrin-binding sialoprotein) sense, 5′-ACAAGCACGCCTACTTCTATCC-3′ and antisense, 5′-CTTCCTCCTCGTCTTCATCACT-3′. The primer set for *GAPDH* (glyceraldehyde-3-phosphate dehydrogenase) was used as an internal standard marker (sense 5′-GGGAAGCTTGTCATCAATGG-3′ and antisense, 5′-GTTGTCATGGATGACCTTGG-3′).

All assays were designed to overlay a junction between two exons to avoid hybridization to genomic DNA. PCR conditions were as follows: 10 min at 95 °C followed by 30 cycles of 30 s at 95 °C, 20 s at 60 °C and 30 s at 72 °C, with a final elongation step of 10 min at 72 °C. Each sample was run in triplicate. Aliquots of PCR products were analysed on 2 % ethidium-bromide-stained agarose gels.

Assay to measure ALP (alkaline phosphatase) activity

ALP activity in osteoblasts was measured using standard methods [11]. Enzyme activity was expressed as units (nmol of *p*-nitrophenol formed/min)/ng of protein. Protein content was determined using the Bio-Rad Laboratories protein assay kit.

Calcium deposition assay

After fixation in paraformaldehyde at room temperature for 1 h, the cells were incubated in 5 % silver nitrate (Wako Pure Chemical) for 1 h under ultraviolet light and rinsed with distilled water. von Kossa staining confirmed black nodules as secretions of the calcified extracellular matrix. To quantify calcium deposition, the cells were washed twice with PBS and treated with 2 M hydrochloric acid overnight. Calcium concentrations in the hydrochloric acid supernatants were determined by the o-cresolphthalein complexone method using the calcium C-test kit (Wako Pure Chemical), normalized to the dish area and expressed as mg/35-mm tissue culture dish. Frozen specimens were cut into 4-μm-thick sections at -20 °C and stained with DAPI (4′6-diamidino-2-phenylindole; Sigma–Aldrich) and von Kossa stains to visualize mineralization. Paraffin specimens were cut into 7-μm-thick sections and stained by von Kossa and counterstained with light-green or Alizarin Red for visualization of mineralization.

Transplantation

All studies were conducted according to the NIH guidelines for the care and treatment of experimental laboratory rodents.

SCID mice (C.B-17/Icr-scid/scidJc1) were purchased from Clea Japan. Diffusion chambers were assembled from commercially available components with a 10-mm inner diameter and 2-mm thickness and membrane filters with a 0.45-μm pore size (Millipore). The filters were attached to both sides of the diffusion chamber with adhesive and sterilized at 80 °C for 24 h. To investigate the calcification of DFOG cells after transplantation, the cells that had not formed a mineralized matrix 4 days after osteogenic induction without 2-glycerophosphate were collected using a cell scraper and transplanted. A suspension of 1×10^6 cells in 100 μl of type 1 collagen gel (Nitta Gelatin) was injected into the diffusion chamber using a syringe and then transplanted into the peritoneal cavity of twelve female mice (7 weeks old; one or two diffusion chamber per mouse). A total of nine diffusion chambers containing cells subjected to osteogenic induction (experimental plots) and the other nine diffusion chambers containing cells without osteogenic induction (control plots) were transplanted into SCID mice. At 4 weeks after transplantation, the diffusion chambers were retrieved, fixed in paraformaldehyde, and embedded in Tissue-Tek OCT™ compound or paraffin.

Statistical analyses

Data were analysed for statistical significance by one-way ANOVA where $P < 0.01$ was considered statistically significant. All experiments were repeated three times.

RESULTS

Isolation of GCs from ovarian follicles

To obtain uniform single-cell fractions of GCs and avoid contamination with TCs (theca cells) and eggs, granulosa layers were extracted from ovarian follicles. These layers were collected and washed three times in PBS by centrifugation. To determine whether the granulosa layer was composed of homogenous GCs, sections of the ovarian follicle and granulosa layer were immunostained with rat anti-(α6 integrin/CD49f) monoclonal antibody. Analysis of the ovarian follicle sections indicated that

the granulosa layer was stained with rat anti-(α6 integrin/CD49f) monoclonal antibody, but the theca layer was not (Figure 1B, a–c). The granulosa layer section was found to be composed of homogeneous GCs (Figure 1B, d–f). The cut granulosa layers were digested with collagenase and gentle agitation. Dissociated GCs were then filtered, washed and centrifuged three times. The isolated GC fraction was immunostained with rat anti-(α6 integrin/CD49f) monoclonal antibody and examined under a fluorescence microscope. Photomicrographs showed that the isolated GC fraction did not contain TCs (Figure 1B, g–i). To ascertain whether these GCs were a homogeneous population, we performed FACS analysis of the GCs after immunostaining with rat anti-(α6 integrin/CD49f) monoclonal antibody and mouse anti-(cytochrome P450 aromatase) antibody. Forward scatter and side scatter analyses showed that the GC fraction was a homogeneous cell population (Figure 1C, a). The results from immunostaining analyses showed a similar pattern and indicated that 90.45 and 99.66 % of the GC fraction were positive for α6 integrin and cytochrome P450 aromatase respectively (Figure 1B, c and d). In addition, 99.66 % of the GC fraction was positive for both α6 integrin and cytochrome P450 aromatase (Figure 1B, b). These results revealed that the GC fraction was a highly homogeneous fraction.

GC dedifferentiation

To confirm the proliferative ability of GCs in plate culture, we performed microscopic observations over 7 days. Immediately after seeding, the primary GCs floated and exhibited a spherical morphology (Figure 2A, a). After 24 h in plate culture, the GCs were strongly attached and began to exhibit an extended cellular morphology (Figure 2A, b). Subsequently, the cytoplasmic rims spread further, and the cell acquired a fibroblastic morphology at 48 h (Figure 2A, c). After 96 h in plate culture, the cells became fibroblast-like in appearance and began proliferating (Figure 2A, d) extensively until confluence (Figure 2A, e). These results indicate that GCs can change their phenotype to become fibroblast-like cells that can proliferate during plate culture. Because these cells had dedifferentiated from homogeneous GCs, we termed them DFOG cells. To examine the changes in the gene expression profile during dedifferentiation, we performed microarray analysis to study the gene expression profile of GC-specific markers in the DFOG cells and compared this profile with that of GC-specific markers in GCs. Microarray analysis detected abundant expression of GC-specific markers including *STAR* (steroidogenic acute regulatory protein), *NR* (nuclear receptor) *0B1*, *CYP19A*, *ESR1* (oestrogen receptor 1), *NR5A1*, *HSD17B1* [hydroxysteroid (17-β) dehydrogenase 1], *NR5A2*, *INHBB*, *LHCGR*, *CYP11A1* (cytochrome P450 family 11 subfamily A1), *FST* (follistatin) and *INHA* (inhibin α) in GCs; the expression of these markers, except *CYP11A1*, decreased on day 1 of culture (Figure 2B). In addition, these markers were not expressed in DFOG cells (Figure 2B). Moreover, expression of genes involved in the regulation of osteogenic differentiation, such as *SP7*, *MGP* (matrix Gla protein), *CDH11* (cadherin 11), *POSTN* (periostin), *DLX5*, *SPP1*, *DCN* (decorin) and *COL1A1* (collagen type I α1), were up-regulated during dedifferentiation, although *BMP* (bone morphogenetic protein) *7*, *BMP3*, *IBSP*, *BGLAP* [bone γ-carboxyglutamate (gla) protein], *ALPL* and *PTHLH* (parathyroid hormone-like hormone) were not expressed (Figure 2B). Other specific genes, such as chondrogenic and neurogenic genes, were also expressed in DFOG cells (see Supplementary Figure S1 at http://www.BiochemJ.org/bj/447/bj4470239add.htm). We next determined the mRNA expression levels of GC-specific and osteogenic genes in GCs and DFOG cells by RT–PCR. Figure 2(C) shows the gene expression pattern of GC-specific and osteogenic markers from the isolated GCs and GCs cultured for 168 h. The density of the amplified cDNA band of some specific markers was normalized to that of the corresponding band of *GAPDH*. In terms of osteogenic genes, mRNA expression of *RUNX2*, *SP7*, *DLX5* and *SPP1* was detected in DFOG cells, but that of *ALP* and *IBSP* was not. None of these markers were detected in GCs; however, expression of GC-specific markers, including *CYP19A3*, *LHCGR* and *INHBB*, were detected. The expression of these markers decreased in DFOG cells (Figure 2). The results of microarray and RT–PCR analyses indicate that GCs dedifferentiate at the gene expression level. We also examined the protein expression levels of GC-specific markers in GCs and DFOG cells by immunofluorescence staining. Expression of α6 integrin and cytochrome P450 aromatase (functional markers of GCs) decreased at the protein level (Figure 2D). These results suggest that DFOG cells lose the functional characteristics of GCs, but acquire the characteristics of osteogenic lineage-committed cells.

Osteogenic differentiation of DFOG cells *in vitro*

The osteogenic differentiation potential of DFOG cells was analysed by culturing the cells under conditions favourable for osteogenic differentiation. BMSCs were used as controls for osteogenic differentiation. ALP activity was analysed by histological staining and spectrophotometry to characterize osteogenic differentiation. DFOG cells before osteogenic induction did not exhibit ALP. When DFOG cells were cultured in the osteogenic induction medium, the cells changed their extended morphology and produced ALP, a characteristic of osteoblasts, from day 4 of culture (Figure 3A, b). By day 4, the increase in ALP activity was rapid and significant ($P < 0.01$), peaking on day 4, and decreasing through the late stages of osteogenesis (Figure 3C). From the beginning of the confluent phase, ALP activity was detected in BMSCs. The ALP activity of BMSCs increased up to day 14 (Figures 3A, e-h and 3C). DFOG cells and BMSCs were also investigated to determine their ability to undergo extracellular matrix mineralization. This mineralization was visualized by von Kossa staining and quantified in the calcium C-test by culturing the cells in the presence of 2-glycerophosphate. Microscopic analysis of DFOG cells confirmed weakly mineralized regions 7 days after osteogenic induction (Figure 3B, c). Bone nodules were observed after 14 days, and their calcium concentrations increased up to day 14 (Figure 3B, d). Matrix mineralization significantly ($P < 0.01$) increased in DFOG cells after osteogenic induction from day 7 to day 14 (Figure 3D). Microscopic analysis of BMSCs confirmed mineralized regions after 14 days, and their calcium concentrations were significant ($P < 0.01$) on day 14 (Figure 3B, h). Osteogenic late-stage differentiation of DFOG cells was evaluated by immunostaining to detect expression of type 1 collagen in the extracellular matrix. Expression of type 1 collagen, an osteoblast-associated matrix protein, has been considered a valid marker of completely differentiated osteoblasts. Microscopic analysis of DFOG cells confirmed expression of type 1 collagen before and after osteogenic induction. Non-fibrillar collagens were observed in the cytoplasm of DFOG cells before osteogenic induction, whereas fibrillar collagens were observed beside the DFOG cells after osteogenic induction (Figure 3E). We next determined the mRNA expression levels of osteogenic genes. Their differentiation markers were analysed by RT–PCR. The osteogenic markers were assessed on days 0, 4, 7 and 14 using cells cultured in OM (osteogenic medium) with 2-glycerophosphate. Figure 4 shows the gene

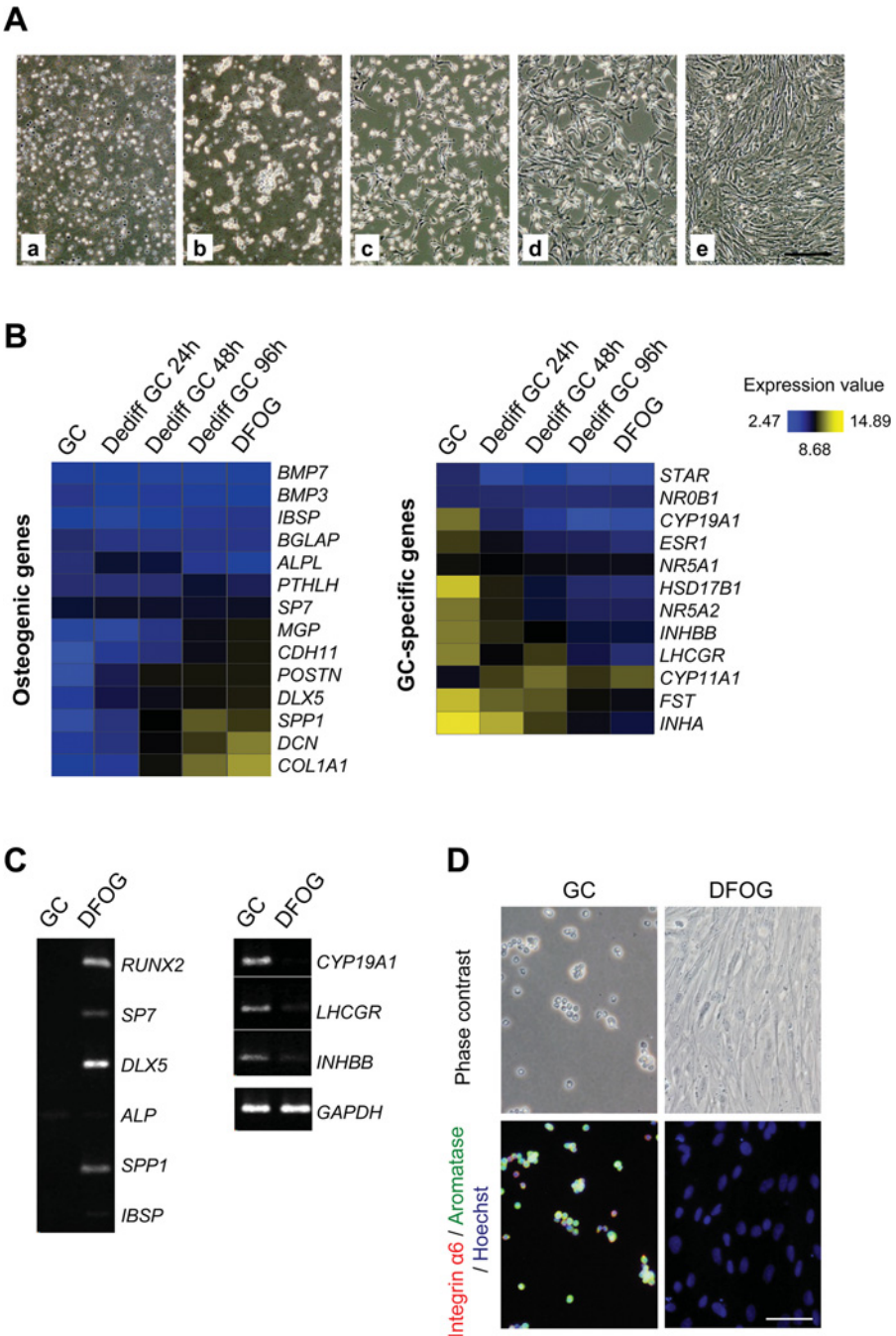

Figure 2 Morphological changes and microarray analyses of dedifferentiation of GCs to DFOG cells by plate culture

(**A**) Phase-contrast microscopy showing morphological changes in plate culture. a, morphology of GCs immediately after isolation. b, morphology of adhered cells on day 1 of culture. c, morphology of extended cells on day 2 of culture. d, the cells changed into fibroblast-like cells and began proliferating on day 4 of culture. e, the cells reached confluence on day 7 of culture. Scale bar = 100 μm. (**B**) Heat map depicting expression levels of mRNAs encoding osteogenic and GC-specific marker genes at each time point during GC dedifferentiation. Yellow and blue indicate higher and lower levels of expression respectively. (**C**) Gene expression patterns of osteogenic and GC-specific markers in GCs and DFOG cells. *RUNX2*, *SP7*, *DLX5*, *ALP*, *SPP1* and *IBSP* were used as osteogenic genes, and *CYP19A1* (aromatase), *LHCGR* and *INHBB* as GC-specific genes. The density of each amplified cDNA band of some osteogenic and GC-specific markers was normalized to that of the corresponding band of *GAPDH*. (**D**) Immunofluorescence using antibodies against α6 integrin/CD49f (red) and cytochrome P450 aromatase (green) in freshly isolated GCs and DFOG cells. Nuclei were visualized with Hoechst stain (blue). Scale bar = 50 μm.

expression patterns of the osteogenic markers during osteogenic differentiation. The density of the amplified cDNA band of some specific markers was normalized to that of the corresponding band of *GAPDH*. From the beginning of the confluent phase, mRNA expression of *RUNX2*, *SP7*, *DLX5* and *SPP1* was detected in DFOG cells. Time-dependent experiments revealed a peak of *ALP* mRNA expression on day 4 during osteogenic differentiation. *SP7* was down-regulated, whereas *RUNX2*, *SPP1* and *IBSP* were up-regulated after osteogenic induction. DFOG cells did not up-regulate expression of GC-specific genes and their differentiation markers after osteogenic induction (see Supplementary Figure S2 at http://www.BiochemJ.org/bj/447/bj4470239add.htm).

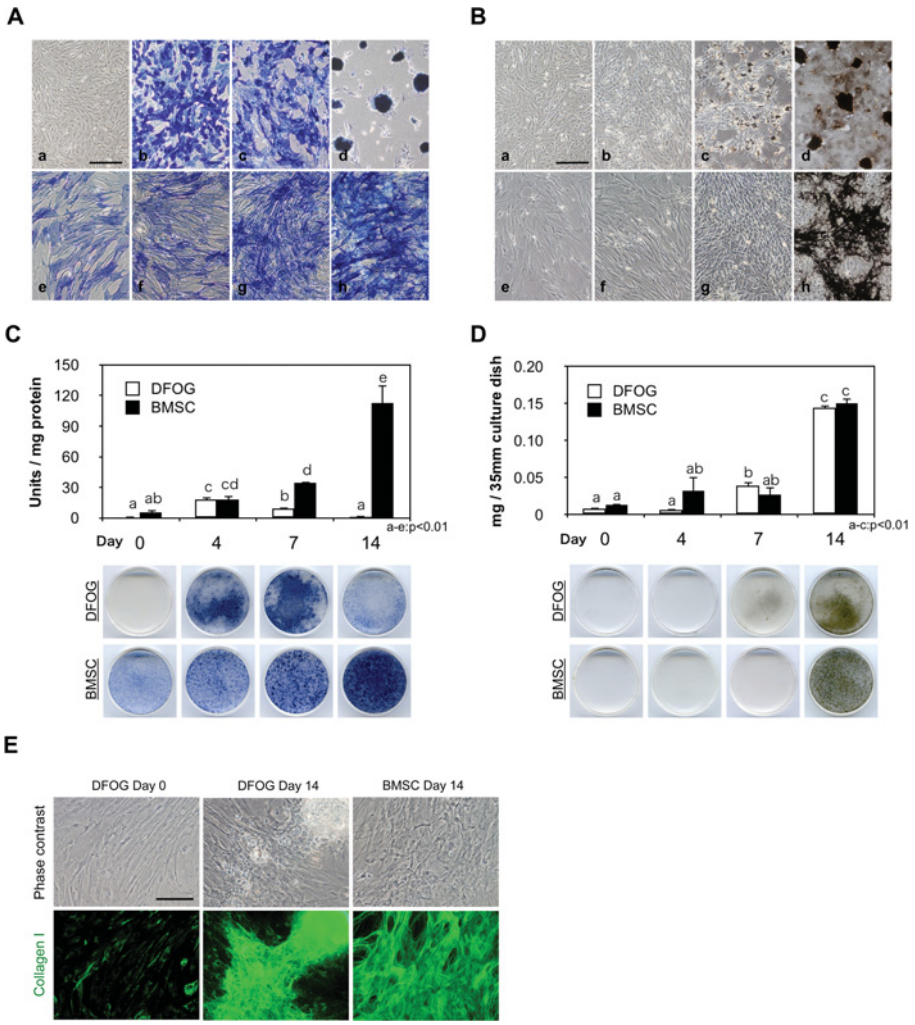

Figure 3 Histological and UV absorbance analyses demonstrating the osteogenic differentiation ability of DFOG cells. BMSCs were prepared as controls for osteoblast differentiation

(**A**) ALP staining after osteogenic induction at various time points. (**B**) von Kossa staining after osteogenic differentiation at different time points. a–d, DFOG cells on days 0, 4, 7 and 14 after osteogenic induction. e–h, BMSCs on days 0, 4, 7 and 14 after osteogenic induction. Magnification = ×10. Scale bar = 100 μm. (**C**) Basal and maximal levels of ALP activity of DFOG cells and BMSCs expressed as units (nmol of *p*-nitrophenol formed/min)/ng of protein. Results are means ± S.D.; $n = 3$. a–e, $P < 0.01$. Significant differences ($P < 0.01$) were observed between a–e. (**D**) Extracellular calcium deposition was measured by the o-cresolphthalein complexone method normalized to the dish area and expressed in mg/35-mm tissue culture dish for DFOG cells and BMSCs. Results are means ± S.D.; $n = 3$. a–c, $P < 0.01$. Significant differences ($P < 0.01$) were observed between a–c. (**E**) Immunofluorescence using antibodies against type I collagen (green) in confluent DFOG cells as well as DFOG cells and BMSCs after osteogenic induction. Scale bar = 100 μm.

CYP19A3, *LHCGR* and *INHBB* were down-regulated in osteogenic culture. From the beginning of the confluent phase, mRNA expression of *RUNX2*, *SP7*, *DLX5*, *ALPL*, *SPP1* and *IBSP* was detected in BMSCs. *SP7* and *DLX5* were down-regulated after osteogenic induction. Time-dependent experiments revealed a peak of *IBSP* mRNA expression on day 4 during osteogenic differentiation. These results indicate that GCs can transdifferentiate into mature osteoblasts *in vitro*.

Formation of osteoid tissue by transplanted DFOG cells

We performed a transplantation experiment using a diffusion chamber system to investigate whether DFOG cells can form osteoid tissue *in vivo*. A total of 18 diffusion chambers were transplanted subcutaneously into mice. At 4 weeks after transplantation, scattered areas of osteoid tissue in all chambers of osteogenic induced DFOG cells were observed after von Kossa (Figure 5A), light green and Alizarin Red staining (Figure 5B), and osteogenic marker proteins were detected by immunostaining of osteocalcin and type 1 collagen (Figure 5B). These results indicate that the osteoid tissue was formed in chambers of osteogenic induced DFOG cells ($n = 9$). The diffusion chamber system showed that osteoid tissues that had formed after transplantation were derived from DFOG cells. The DFOG cells were subcutaneously implanted into the host animals and were distinguished from the host cells using a filter. Osteogenic induced DFOG cells that were cultured without 2-glycerophosphate prior to injection formed osteoid tissue in the diffusion chambers at the transplantation site, whereas control cells did not (Figure 5A). Taken together, these results indicate that DFOG cells can form ectopic osteoid tissue in the absence of host cells.

DISCUSSION

In the present paper, we have reported that porcine ovarian follicle-derived DFOG cells possess most of the characteristics

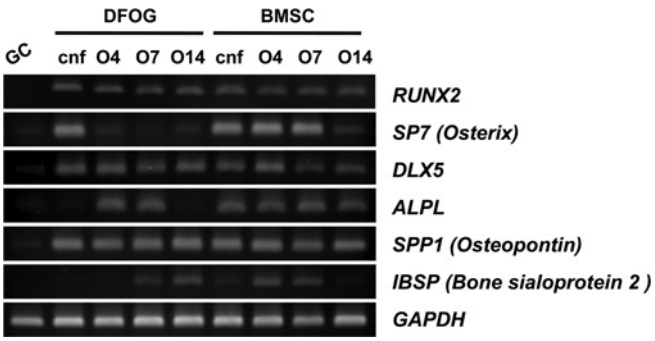

Figure 4 Gene expression patterns of osteogenic markers before and after osteogenic induction

Total RNA was extracted from GCs immediately after isolation and from DFOG cells before and after osteogenic induction. BMSCs were prepared as controls for osteoblast differentiation. The O4, O7 and O14 samples were collected on days 4, 7 and 14 after osteogenic induction respectively. The time-dependent effect of transdifferentiation on mRNA expression of osteogenic transcription factors (*RUNX2*, *SP7* and *DLX5*) and osteoblastic functional markers (*ALPL*, *SPP1* and *IBSP*). The density of each amplified cDNA band of some osteogenic markers was normalized to that of the corresponding band of *GAPDH*. cnf, confluence.

of osteoblasts *in vitro*. Moreover, DFOG cells subcutaneously transplanted into SCID mice could differentiate into mature osteoblasts and, even more surprisingly, form osteoid tissue. Thus GCs might be useful for studying transdifferentiation of mammalian cells.

The ovary is composed of the following three distinct regions: an outer cortex containing the germinal epithelium and follicles, a central medulla consisting of the stroma, and a hilum around the area of attachment of the ovary to the mesovarium [18]. Steroidogenic cells of the ovary are GCs, which are located in avascular cellular compartments surrounding the oocyte, and TCs, which reside in the ovarian stroma. These two cellular compartments are separated by the basal lamina [19]. The possible contamination of GC populations with stromal cells such as TCs was an important concern during the present study. GCs and TCs can be distinguished by expression of α6 integrin/CD46f [15]. To determine whether the cells isolated from the ovarian follicles were GCs, primary cells were analysed by microscopy. Microscopic analysis of isolated cells immunostained with rat anti-(α6 integrin/CD49f) monoclonal antibody demonstrated that all cells were GCs (Figure 2A), indicating that all cells within the centrifugal cell fraction are GCs and not TCs. The major functions of GCs include production of sex steroids as well as myriad growth factors, which are believed to interact with the oocyte during its development. Sex steroid production is characterized by stimulation of GCs by FSH to convert androgens (coming from TCs) into oestradiol by aromatase during the follicular phase of the menstrual cycle [20]. FACS analysis was performed to investigate the homogeneity of the isolated GCs. In fact, 99.66 % of the GC fraction was positive for both α6 integrin and cytochrome P450 aromatase (Figure 1B, b). Considering these results, our findings indicate that the cell fraction isolated by enzymatic digestion and multiple rounds of centrifugation and filtration consisted of a homogeneous GC population.

Several hundred thousand GCs exert a multitude of specialized functions encompassing the ultimate function of the follicle, including producing large amounts of oestradiol, adapting FSH and luteinizing hormone receptivity to the endocrine milieu, nursing the oocyte, and communicating with both the enclosed oocyte and surrounding TCs [21,22]. Thus GCs are considered to be completely differentiated. In the present study, we found that GCs can change their phenotype to become fibroblast-like cells that are able to proliferate during plate culture (Figure 2A). Microarray assays revealed that the cells gradually started to express osteogenic genes, whereas expression of GC-specific genes decreased (Figure 2B). The results of the present study revealed that GCs enter the cell cycle, dedifferentiate into fibroblast-like DFOG cells and acquire osteoblastic potential when subjected to plate culture in the absence of any special factors.

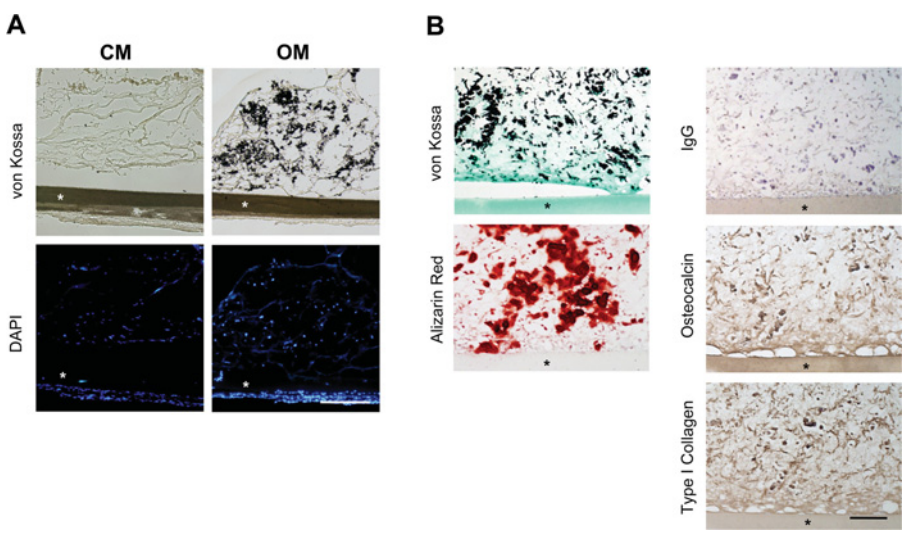

Figure 5 Osteoid tissue formation by transplanted DFOG cells

(**A**) Frozen sections were stained with DAPI and von Kossa stains to visualize mineralization. DFOG cells maintained in control medium (CM) before transplantation formed only fibrous connective tissue, however, the cells cultured in OM without 2-glycerophosphate before transplantation generated a mineralized bone matrix in the diffusion chamber. (**B**) Paraffin sections of OM were stained by von Kossa and counterstained with light green or Alizarin Red for visualization of mineralization. Osteocalcin and type 1 collagen as osteogenic marker proteins were immunostained using the ABC method and counterstained with haematoxylin. IgG was used as a negative control. *, filter membrane. Scale bar = 100 μm.

To confirm the osteogenic potency of DFOG cells, we first examined typical osteogenic markers of osteoblasts. Osteoblastic differentiation *in vitro* is marked by three distinct stages of cellular activity: proliferation, extracellular matrix maturation and matrix mineralization [23]. As cells form multilayered clusters, the proliferation rate decreases and expression of the bone/liver/kidney isoform of ALP (ALPL) increases [24–26]. Following the period of matrix maturation, nodule cells begin to mineralize the extracellular matrix. Expression levels of osteocalcin and BSP (bone sialoprotein) increases with mineral deposition [24,27], whereas those of ALP decline [25,26] in the primary osteoblasts. *ALP* and *BSP* mRNA expression patterns in DFOG cells in the present study (Figure 4) were very similar to those previously reported, suggesting that DFOG cells accomplish a normal osteogenic differentiation similar to that accomplished by the primary osteoblasts. However, although the cause was unknown, BMSCs showed decreased *IBSP* mRNA expression on day 14. OSX (osterix) is an osteoblast-specific transcription factor required for osteogenic differentiation and bone formation. Osx-null mice develop a normal cartilage skeleton, but fail to form bone and express osteogenic marker genes [28]. DFOG cells newly express *ALP* and *BSP* mRNA after *OSX* mRNA expression decreases. Moreover, a decrease in *OSX* mRNA expression was revealed in time-dependent experiments with BMSCs (Figure 4). We previously reported that dedifferentiated adipocytes (DFAT cells) showed decreased *OSX* mRNA expression, which was transient in the osteogenic differentiation process [11]. From these results, it appears that OSX may not be indispensable for osteogenic late-phase differentiation. To confirm the chondrogenic differentiation of DFOG cells after osteogenic induction, we examined typical chondrogenic markers such as Sox9 [SRY (sex determining region Y)-box 9], type 2 collagen and ACAN (aggrecan) (see Supplementary Figure S3 http://www.BiochemJ.org/bj/447/bj4470239add.htm). As a result, although GC had expressed Sox9 after dedifferentiation, the expression level of Sox9 decreased in DFOG cells after osteogenic induction. Col2a1 (type 2 collagen $\alpha 1$) and ACAN were not expressed in DFOG cells before/after osteogenic induction. From these results, DFOG cells did not differentiate into chondrocytes.

Scaffolds or layers of calcium phosphate are widely used as biomaterials in bone tissue engineering. Several investigations have shown that calcium phosphate surfaces have a beneficial effect on bone osteogenesis *in vivo* [29–31]. These reports cannot rule out the possibility that recipient-derived cells are involved in the transplantation of scaffolds for bone regeneration. Sun et al. [32] reported that vascularization of transplanted bone tissue can occur by the ingrowth of host blood vessels or can originate within transplanted bone tissue. Yamaguchi et al. [33] demonstrated that the bone marrow stromal cell line ST2 forms mineralized bone tissue in diffusion chambers after transplantation. Their results suggest that ST2 cells could mineralize bone tissue without recruiting host animal-derived mesenchymal stem cells and osteoblasts. We applied this technique to investigate the osteogenic potency of DFOG cells *in vivo*. Our diffusion chamber model revealed that DFOG cells mineralized the bone matrix without host cell recruitment. Only after osteogenic induction for 4 days *in vitro* before transplantation, DFOG cells formed osteoid tissue *in vivo* after transplantation (Figure 5). Because osteoid tissue was observed in DFOG cells cultured without 2-glycerophosphate (Figure 5), exogenous calcium phosphate was not required. These results indicate that DFOG cells were completely converted into mature osteoblasts *in vivo* after osteogenic induction.

Previously, Kossowska-Tomaszczuk et al. [16] reported that human luteinizing GCs that grew in the presence of LIF were differentiated into other cell lineages, such as osteoblasts, chondrocytes and neurons. Freshly collected luteal phase GCs expressed OCT4 [octamer-binding protein 4; *POU5F1* (POU class 5 homeobox 1)], a typical embryonic stem cell marker, throughout their culture in the presence of LIF. In contrast, we found that freshly collected follicular-phase GCs presented abundant GC-specific markers, but stem cell marker genes such as *POU5F1* mRNA were not expressed (see Supplementary Figure S1). The GCs gradually decreased expression of GC-specific genes during culture when the expression of various other cell-specific genes, including osteogenic genes, began (Figures 2B and 2C). Moreover, GCs that expressed osteogenic genes were completely differentiated into mature osteoblasts *in vitro* (Figures 3 and 4) and *in vivo* (Figure 5). From these reports and results, we suggest that osteogenesis of cultured GCs is unrelated to the menstrual cycle, i.e. to the follicular and luteal phases. Taken together, these findings indicate that GCs can transdifferentiate into osteoblasts not as stem cells, but as functional differentiating cells both *in vitro* and *in vivo*.

Reviews of reported cases of bone in the ovary imply several trends in the pathological conditions of the ovary in which the heterotopic bone is found. In the review by Shipton and Meares [35], the most common ovarian diagnoses associated with bone formation were endometriosis, fibromas and serous cystadenomas. In the majority of the reported cases in which histological details are described, the bone primarily occurs in the stroma of cyst walls [35,36]. On the basis of these reports [35–37], Zahn and Kendall [34] suggested that development of bone results from a metaplastic process in the stroma. Gerbie et al. [37] presented an excellent summary of theories explaining heterotopic bone formation, suggesting that osteoblasts may differentiate from fibroblasts and that conditions in the connective tissue must be favourable for ossification. In their report, almost all cases were associated with either chronic inflammation or endometriosis, suggesting that these conditions may serve as a stimulus for a heterotopic process. In the present study, we demonstrated that GCs derived from ovary follicles were converted into osteoblasts. The GCs changed their phenotype to fibroblast-like cells during plate culture (Figure 2A). They also acquired the characteristics of osteogenic lineage-committed cells. On the basis of these results, we speculated that DFOG cells have a similar status to fibroblast-like cells in the stroma of cyst walls. Disruption of the surrounding matrix of GCs by collagenase treatment and the morphological change to a fibroblast-like cell by plate culture, as performed during the experiments of the present study, may lead to conditions such as chronic inflammation and endometriosis.

In conclusion, our observations indicate that GCs can dedifferentiate into fibroblast-like DFOG cells that possess the potential to differentiate into osteogenic lineages similar to DFAT cells. Although much research on cell reprogramming with respect to a cell source for regenerating organs has focused on urodele amphibians and zebrafish, we focused on multipotent cells generated from fully differentiated cells, such as GCs and adipocytes in mammals. Studies of these cellular models may provide a novel approach for studying reprogramming of the mammalian cell. Because DFOG and DFAT cells are easily isolated from a small amount of tissue and are readily expanded with high purity, DFOG and DFAT cells may be applicable to many tissue engineering strategies and cell-based therapies. However, why these cells have multipotency remains unclear. The understanding of the mechanism by which DFOG and DFAT cells acquire their multipotency is an important concern. Our future research will search for a common driving factor for dedifferentiation and the multipotency acquisition mechanism of mammalian cells using DFOG and DFAT cells. Moreover, we will eventually understand

the molecular basis of transdifferentiation in our model systems where transdifferentiation occurs in an appropriate condition, and thereby be able to develop new therapies for stimulating regeneration in higher mammals, including humans.

AUTHOR CONTRIBUTION

Yoshinao Oki performed most of the experimental work and wrote the paper; Hiromasa Ono, Nobuki Sugiura, Takeharu Motohashi and Hiroyuki Nobusue helped to develop and performed some of the experimental work; Hiromasa Ono helped to review the paper prior to submission; Koichiro Kano initiated and oversaw the study and revised the paper and all authors contributed to and have approved the paper.

ACKOWLEDGEMENTS

We are grateful to Chihiro Kaneko for technical assistance.

FUNDING

This work was supported by Okinawa Research and Industrialization Project for the Forefront Medical Care. K.K. was also supported by the Ministry of Education, Science, Sports, and Culture of Japan [grant number 22580340].

REFERENCES

1 Okada, T. S. (1991) Transdifferentiation. Flexibility in Cell Differentiation, Clarendon Press, Oxford
2 Tsonis, P. A., Madhavan, M., Tancous, E. E. and Del Rio-Tsonis, K. (2004) A newt's eye view of lens regeneration. Int. J. Dev. Biol. **48**, 975–980
3 Henry, J. J. (2003) The cellular and molecular bases of vertebrate lens regeneration. Int. Rev. Cytol. **228**, 195–265
4 Araki, M. (2007) Regeneration of the amphibian retina: role of tissue interaction and related signaling molecules on RPE transdifferentiation. Dev. Growth Differ. **49**, 109–120
5 Grogg, M. W., Call, M. K. and Tsonis, P. A. (2006) Signaling during lens regeneration. Semin. Cell Dev. Biol. **17**, 753–758
6 Nye, H. L., Cameron, J. A., Chernoff, E. A. and Stocum, D. L. (2003) Regeneration of the urodele limb: a review. Dev. Dyn. **226**, 280–294
7 Brockes, J. P. and Kumar, A. (2002) Plasticity and reprogramming of differentiated cells in amphibian regeneration. Nat. Rev. Mol. Cell Biol. **3**, 566–574
8 Frid, M. G., Kale, V. A. and Stenmark, K. R. (2002) Mature vascular endothelium can give rise to smooth muscle cells via endothelial–mesenchymal transdifferentiation: *in vitro* analysis. Circ. Res. **90**, 1189–1196
9 Shen, C. N., Horb, M. E., Slack, J. M. and Tosh, D. (2003) Transdifferentiation of pancreas to liver. Mech. Dev. **120**, 107–116
10 Li, W. C., Horb, M. E., Tosh, D. and Slack, J. M. (2005) *In vitro* transdifferentiation of hepatoma cells into functional pancreatic cells. Mech. Dev. **122**, 835–847
11 Oki, Y., Watanabe, S., Endo, T. and Kano, K. (2008) Mature adipocyte-derived dedifferentiated fat cells can trans-differentiate into osteoblasts *in vitro* and *in vivo* only by all-*trans* retinoic acid. Cell Struct. Funct. **33**, 211–222
12 Kazama, T., Fujie, M., Endo, T. and Kano, K. (2008) Mature adipocyte-derived dedifferentiated fat cells can transdifferentiate into skeletal myocytes *in vitro*. Biochem. Biophys. Res. Commun. **377**, 780–785
13 Matsumoto, T., Kano, K., Kondo, D., Fukuda, N., Iribe, Y., Tanaka, N., Matsubara, Y., Sakuma, T., Satomi, A., Otaki, M. et al. (2008) Mature adipocyte-derived dedifferentiated fat cells exhibit multilineage potential. J. Cell. Physiol. **215**, 210–222
14 Ohta, Y., Takenaga, M., Tokura, Y., Hamaguchi, A., Matsumoto, T., Kano, K., Mugishima, H., Okano, H. and Igarashi, R. (2008) Mature adipocyte-derived cells, dedifferentiated fat cells (DFAT), promoted functional recovery from spinal cord injury-induced motor dysfunction in rats. Cell Transplant. **17**, 877–886
15 Fujiwara, H., Ueda, M., Takakura, K., Mori, T. and Maeda, M. (1995) A porcine homolog of human integrin alpha 6 is a differentiation antigen of granulosa cells. Biol. Reprod. **53**, 407–417
16 Kossowska-Tomaszczuk, K., De Geyter, C., De Geyter, M., Martin, I., Holzgreve, W., Scherberich, A. and Zhang, H. (2009) The multipotency of luteinizing granulosa cells collected from mature ovarian follicles. Stem Cells **27**, 210–219
17 Chan, W. K. and Tan, C. H. (1986) FSH-induced aromatase activity in porcine granulosa cells: non-competitive inhibition by non-aromatizable androgens. J. Endocrinol. **108**, 335–341
18 Carr, B. R. (1998) Uniqueness of oral contraceptive progestins. Contraception **58**, 23S–27S
19 Weakley, B. S. (1966) Electron microscopy of the oocyte and granulosa cells in the developing ovarian follicles of the golden hamster (*Mesocricetus auratus*). J. Anat. **100**, 503–534
20 Garzo, V. G. and Dorrington, J. H. (1984) Aromatase activity in human granulosa cells during follicular development and the modulation by follicle-stimulating hormone and insulin. Am. J. Obstet. Gynecol. **148**, 657–662
21 Gougeon, A. (1996) Regulation of ovarian follicular development in primates: facts and hypotheses. Endocr. Rev. **17**, 121–155
22 Niswender, G. D., Juengel, J. L., Silva, P. J., Rollyson, M. K. and McIntush, E. W. (2000) Mechanisms controlling the function and life span of the corpus luteum. Physiol. Rev. **80**, 1–29
23 Lian, J. B. and Stein, G. S. (1992) Concepts of osteoblast growth and differentiation: basis for modulation of bone cell development and tissue formation. Crit. Rev. Oral Biol. Med. **3**, 269–305
24 Owen, T. A., Aronow, M., Shalhoub, V., Barone, L. M., Wilming, L., Tassinari, M. S., Kennedy, M. B., Pockwinse, S., Lian, J. B. and Stein, G. S. (1990) Progressive development of the rat osteoblast phenotype *in vitro*: reciprocal relationships in expression of genes associated with osteoblast proliferation and differentiation during formation of the bone extracellular matrix. J. Cell. Physiol. **143**, 420–430
25 Turksen, K. and Aubin, J. E. (1991) Positive and negative immunoselection for enrichment of two classes of osteoprogenitor cells. J. Cell Biol. **114**, 373–384
26 Malaval, L., Modrowski, D., Gupta, A. K. and Aubin, J. E. (1994) Cellular expression of bone-related proteins during *in vitro* osteogenesis in rat bone marrow stromal cell cultures. J. Cell. Physiol. **158**, 555–572
27 Pockwinse, S. M., Wilming, L. G., Conlon, D. M., Stein, G. S. and Lian, J. B. (1992) Expression of cell growth and bone specific genes at single cell resolution during development of bone tissue-like organization in primary osteoblast cultures. J. Cell. Biochem. **49**, 310–323
28 Nakashima, K., Zhou, X., Kunkel, G., Zhang, Z., Deng, J. M., Behringer, R. R. and de Crombrugghe, B. (2002) The novel zinc finger-containing transcription factor osterix is required for osteoblast differentiation and bone formation. Cell **108**, 17–29
29 Lee, Y. M., Park, Y. J., Lee, S. J., Ku, Y., Han, S. B., Choi, S. M., Klokkevold, P. R. and Chung, C. P. (2000) Tissue engineered bone formation using chitosan/tricalcium phosphate sponges. J. Periodontol. **71**, 410–417
30 Uemura, T., Dong, J., Wang, Y., Kojima, H., Saito, T., Iejima, D., Kikuchi, M., Tanaka, J. and Tateishi, T. (2003) Transplantation of cultured bone cells using combinations of scaffolds and culture techniques. Biomaterials **24**, 2277–2286
31 Mauney, J. R., Jaquiery, C., Volloch, V., Heberer, M., Martin, I. and Kaplan, D. L. (2005) *In vitro* and *in vivo* evaluation of differentially demineralized cancellous bone scaffolds combined with human bone marrow stromal cells for tissue engineering. Biomaterials **26**, 3173–3185
32 Sun, H., Qu, Z., Guo, Y., Zang, G. and Yang, B. (2007) *In vitro* and *in vivo* effects of rat kidney vascular endothelial cells on osteogenesis of rat bone marrow mesenchymal stem cells growing on polylactide-glycoli acid (PLGA) scaffolds. Biomed. Eng. Online **6**, 41
33 Yamaguchi, A., Ishizuya, T., Kintou, N., Wada, Y., Katagiri, T., Wozney, J. M., Rosen, V. and Yoshiki, S. (1996) Effects of BMP-2, BMP-4, and BMP-6 on osteoblastic differentiation of bone marrow-derived stromal cell lines, ST2 and MC3T3-G2/PA6. Biochem. Biophys. Res. Commun. **220**, 366–371
34 Zahn, C. M. and Kendall, B. S. (2001) Heterotopic bone in the ovary associated with a mucinous cystadenoma. Mil. Med. **166**, 915–917
35 Shipton, E. A. and Meares, S. D. (1965) Heterotopic bone formation in the ovary. Aust. N.Z. J. Obstet. Gynaecol. **90**, 100–102
36 Barua, R. and Cox, L. W. (1982) Occurrence of bone in serous cystadenocarcinoma of the ovary. Aust. N.Z. J. Obstet. Gynaecol. **22**, 183–186
37 Gerbie, A. B., Greene, R. R. and Reis, R. A. (1958) Heteroplastic bone and cartilage in the female genital tract. Obstet. Gynecol. **11**, 573–578

Received 30 January 2012/9 July 2012; accepted 27 July 2012
Published as BJ Immediate Publication 27 July 2012, doi:10.1042/BJ20120172

Biochem. J. (2012) **447**, 239–248 (Printed in Great Britain) doi:10.1042/BJ20120172

SUPPLEMENTARY ONLINE DATA

Dedifferentiated follicular granulosa cells derived from pig ovary can transdifferentiate into osteoblasts

Yoshinao OKI, Hiromasa ONO, Takeharu MOTOHASHI, Nobuki SUGIURA, Hiroyuki NOBUSUE and Koichiro KANO[1]

Laboratory of Cell and Tissue Biology, College of Bioresource Sciences, Nihon University, 1866 Kameino, Fujisawa 252-0880, Japan

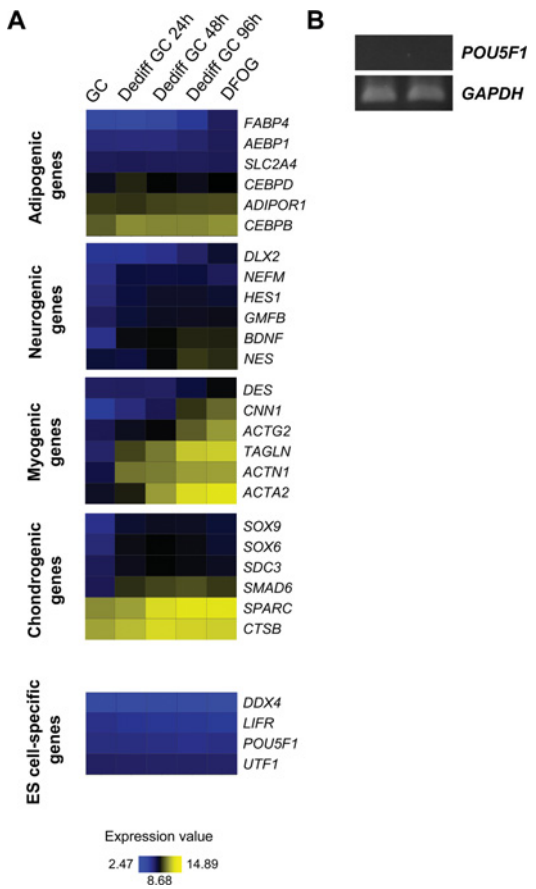

Figure S1 Microarray analysis during dedifferentiation of GCs to DFOG cells and RT–PCR analysis of OCT4 (*POU5F1*) by plate culture

(**A**) Heat map depicting expression levels of mRNAs encoding adipogenic, neurogenic, myogenic, chondrogenic and embryonic stem cell-specific marker genes at each time point during GC dedifferentiation (Dediff). Yellow and blue indicate higher and lower levels of expression respectively. *ACTG2*, actin, $\gamma 2$, smooth muscle, enteric; *ACTN*, actinin α; *ADIPOR1*, adiponectin receptor 1; *AEBP1*, AE-binding protein 1; *BDNF*, brain-derived neurotrophic factor; *CEBPB*, CAAT/enhancer-binding protein (C/EBP), β; *CEBPD*, CCAAT/enhancer-binding protein (C/EBP), δ; *CNN1*, calponin 1, basic, smooth muscle; *CTSB*, cathepsin B; *DDX4*, DEAD (Asp-Glu-Ala-Asp) box polypeptide 4; *DES*, desmin; *FABP4*, fatty acid-binding protein 4, adipocyte; *GMFB*, glia maturation factor β; *HES1*, hairy and enhancer of split 1, (*Drosophila*); *NEFM*, neurofilament, medium polypeptide; *NES*, nestin; *SDC3*, syndecan 3; *SLC2A4*, solute carrier family 2 (facilitated glucose transporter), member 4; *SPARC*, secreted protein, acidic, cysteine-rich (osteonectin); *TAGLN*, transgelin; *UTF1*, undifferentiated embryonic cell transcription factor 1. (**B**) Expression of the *POU5F1* gene in GCs and DFOG cells. The primer sets for *POU5F1* used were: forward, 5′-GCTGACAACAACGAGAATCTGC-3′ and reverse, 5′-ACGCGGACCACATCCTTCTCTAG-3′ [1]. The density of each amplified cDNA band of *POU5F1* was normalized to that of the corresponding band of *GAPDH*.

[1] To whom correspondence should be addressed (email kkano@brs.nihon-u.ac.jp).

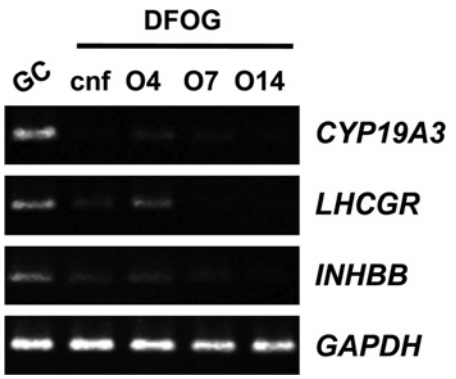

Figure S2 Gene expression patterns of GC-specific markers before and after osteogenic induction

Total RNA was extracted from GCs immediately after isolation and from DFOG cells before and after osteogenic induction. The O4, O7 and O14 samples were collected on days 4, 7 and 14 after osteogenic induction respectively. The time-dependent effect of transdifferentiation on mRNA expression of GC-specific markers, namely *CYP19A3*, *LHCGR* and *INHBB*. After osteogenic induction, expression of GC-specific marker genes was lost. The density of each amplified cDNA band of some GC-specific markers was normalized to that of the corresponding band of *GAPDH*. cnf, confluence.

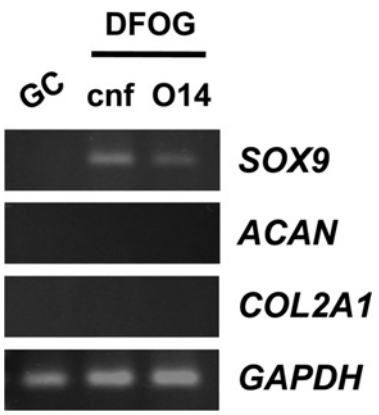

Figure S3 Gene expression patterns of chondrogenic markers before and after osteogenic induction

Total RNA was extracted from GCs immediately after isolation and from DFOG cells before and after osteogenic induction. The O14 samples were collected on day 14 after osteogenic induction. The time-dependent effect of transdifferentiation on mRNA expression of chondrogenic markers, namely *SOX9*, *ACAN* and *COL2A1*. The density of each amplified cDNA band of some chondrogenic markers was normalized to that of the corresponding band of *GAPDH*. The primer sets for chondrogenic genes used were: *SOX9* forward, 5′-CTGAAGAAGGAGAGCGAAGAGG-3′ and reverse 5′-AGATGGCGTTGGGAGAGATG-3′; *ACAN* forward, 5′-AAGAGATGCCAACAGCCAAAC-3′ and reverse, 5′-TGTCGTTCAAGCCAATCCAC-3′; and *COL2A1* forward, 5′-CATTGCCTACCTGGACGAAG-3′ and reverse, 5′-GGATTGTGTTGTTTCTGGGTTC-3′. cnf, confluence.

REFERENCE

1 Ezashi, T., Telugu, B. P., Alexenko, A. P., Sachdev, S., Sinha, S. and Roberts, R. M. (2009) Derivation of induced pluripotent stem cells from pig somatic cells. Proc. Natl. Acad. Sci. U.S.A. **106**, 10993–10998

Received 30 January 2012/9 July 2012; accepted 27 July 2012
Published as BJ Immediate Publication 27 July 2012, doi:10.1042/BJ20120172